Differential Sensors in Substrate Integrated Waveguide Technology Loaded with Complementary Split-Ring Resonators for Liquid Characterization

Víctor García, Yolanda Campos-Roca, and Alfonso Gómez García

***Abstract*— This paper presents three low-cost microwave permittivity sensors for dielectric characterization of liquids. The sensors are based on a differential design concept to achieve robust performance in relation to fluctuations of the environmental parameters (humidity and temperature). The three circuits are implemented on substrate integrated waveguide technology loaded with two complementary split ring resonators (CSRRs). By incorporating three plated via-holes between them, the CSRRs can be effectively decoupled while maintaining a compact design. The sensors, operating in C band, are manufactured by laser etching on a standard printed circuit board process using an RO4003C substrate. They have two ports and do not require surface-mount soldering of discrete components. Sensors with different CSRR geometries (rectangular double ring, circular double ring and circular triple ring) are analyzed by electromagnetic simulations and measurements. The measured results show good agreement in comparison to the simulations. Furthermore, the sensing performance is experimentally assessed by applying them to the dielectric characterization of deionized water and ethanol solutions with different concentrations, using capillary glass tubes as sample containers. The highest average measured frequency sensitivity achieved is 12.24 MHz per unit change in real permittivity with the sensor based on circular double ring CSRRs, and it is obtained with a very small liquid sample volume of about 1.5µL.**

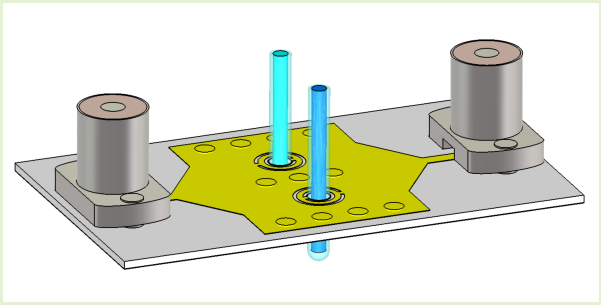

***Index Terms*— Complementary Split Ring Resonator (CSRR), dielectric characterization of liquids, differential microwave sensor, Substrate Integrated Waveguide (SIW).**

I. Introduction

MICROWAVE sensing to determine liquid composition is receiving increasing attention in different application areas, such as food quality assessment [1], detection of water pollution [2], the biological, biomedical and pharmaceutical fields [3], [4], and the chemical industry [5]. In comparison to chemical procedures, microwave based sensing offers the advantage of real-time monitoring. For example, [6] shows that the microwave sensor proposed for fermentation monitoring is capable of real-time operation without interruption in the process, whereas other alternative techniques such as CO2 production measurement would require a considerable amount of time to analyze samples. The sensing principle is based on the relationship between the dielectric constant of the liquid under test (LUT) and its composition. A variation in the sample dielectric permittivity affects the electromagnetic (EM) response of the sensor and can be used to detect the composition. For instance, since water has higher permittivity than ethanol, binary mixtures of water and ethanol will exhibit a reduction in permittivity as the ethanol concentration increases [7].

Different microwave methods and technologies have been proposed to measure the dielectric permittivity of liquids [8]. An initial classification can distinguish between two broad categories: non-planar versus planar. In comparison to non-planar technologies, such as open-ended coaxial probes,

Manuscript received xxxxxx, xxx . This research has been partially supported by: the Spanish Ministry of Science, Innovation and Universities under the State Subprogram for Research Infrastructures and Scientific-Technical Equipment (Grant EQC2019-005583-P); the Spanish Government under grant PID2021-122856NB-C21, funded by MCIN/AEI/10.13039/501100011033 (Agencia Estatal de Investigación), by EU (European Union) "NextGenerationEU"/PRTR and by European Regional Development Fund (ERDF) A Way of making Europe (FEDER, EU); Víctor García was supported by Junta de Extremadura, Spain (Project TE-0041-21) and he is currently supported by a predoctoral FPI grant funded by MCIN/AEI/ 10.13039/501100011033 and by "ESF Investing in your future".

Víctor García, Yolanda Campos-Roca and Alfonso Gómez García are with the Department of Computer and Communication Technologies, Universidad de Extremadura, Avenida de las Letras, s/n, 10003, Cáceres, Spain (e-mail: victorgg@unex.es; ycampos@unex.es; alfonsogg@unex.es).

waveguide cavities or free-space measurements, planar sensors have the advantage of their compact size, low-cost and ease of fabrication. In addition, they are easier to integrate with other circuit components. [9] is a recent comprehensive review on planar microwave sensors. Also, microwave sensors can be classified according to their resonant or non-resonant operation. The resonant technique is narrowband and it is based on the change of the resonant parameters due to the interaction of the sensor with the LUT. Its main advantages are high accuracy and sensitivity. In this context, frequency-variation approaches have been proposed based on several common sensing elements, such as split ring resonators (SRRs) [10], [11], complementary SRRs (CSRRs) [12], [13], [14], [15], complementary electric-LC resonators [14], or spoof surface plasmon polaritons [16], among others. Other operating principles of resonant sensors are amplitude variation [17] or phase-variation [18]. Most of the planar resonant sensors presented in the scientific literature are implemented using microstrip technology. However, substrate integrated waveguide (SIW) is a convenient alternative for this purpose due to its high unloaded quality factor and low losses [19], [20], [21]. This technology can be combined with metamaterial-inspired unit cells etched on the top surface of the SIW to obtain high sensitivity sensors with a very compact size [22].

A common limitation of many of the proposed permittivity sensors for liquid characterization is cross-sensitivity to environmental conditions (temperature, humidity, etc.) which may lead to sensor miscalibration. In [23], the authors explain that the resonance frequency of a microwave planar sensor is dependent not only on the measurand, but also on the permittivity of the substrate, which leads to potential cross-sensitivities in the case of environmental fluctuations. Robustness against these environmental variations can be enhanced through the use of differential sensors. This approach is generally based on two elements, one of which operates as the sensing component whereas the other is regarded as the reference. In the previously cited work [23], the authors proposed a differential sensor design concept based on transmission, implemented in microstrip technology loaded with stepped-impedance resonators. Another example is the differential sensor presented in [24], which was based on frequency splitting. It used a splitter/combiner configuration loaded with a pair of identical SRRs. Some of the published differential sensors offer high accuracy and sensitivity based on structures with three [25] or four ports [26], [27], which require complicated measurement set-ups. Other examples include discrete surface-mounted elements, such as the sensors proposed in [28], [29] and [30]. In some cases, there is some coupling between resonators that may have a negative impact on the performance [31]. To avoid these limitations, some proposals have been presented in the scientific literature. Recently, two-port differential designs have been reported that are based on circular spiral resonators (CSRs) [32] and stepped-impedance resonators [33], in microstrip technology. One of the scientific challenges to face in this research line is to increase sensitivity using the minimum amount of LUT volume. Hence, the main objective of this work was to explore new design approaches that demonstrate improved sensitivity per unit volume with respect to the state-of-the-art, under conditions of low-cost manufacturing and simple test.

The three sensors for liquid characterization presented in this article are based on a SIW structure loaded with two CSRRs that are uncoupled through the use of three plated via-holes. The sensing performance, that is based on the reflection operation, uses the difference between S_{11} and S_{22}. To the authors' best knowledge, this design approach has not been previously published. Manufacturing is based on standard printed circuit board (PCB) technology, and it does not require surface-mounting of discrete components, so it is low-cost and simple. Furthermore, the two-port configuration allows for easy testing.

The structure of the paper is as follows. Section II presents the operation principle and design approach. Three different geometries for the implementation of the CSRRs have been optimized and tested by numerical simulations with CST Microwave Studio. These geometries are the following: rectangular double ring, circular double ring and circular triple ring. The three sensors have been manufactured and the experimental results are presented in section III. Validation of the EM simulation methodology is addressed through tolerance analyses performed with CST on the three bare designs, taking the main manufacturing uncertainties into account (subsection III-A). Next, the circuits have been tested by loading them with mixtures of deionized (DI) water and ethanol. A comparison with the state-of-the-art is included based on the most commonly used quantitative metrics (subsection III-B). This comparison highlights the performance advantages of the proposed design concept in terms of frequency sensitivity per unit volume of LUT. Finally, section IV draws the conclusion.

II. Operation Principle and Sensor Design

The design concept is based on a SIW transmission line loaded with two uncoupled CSRRs to achieve differential detection. Fig. 1 shows the top views of the 3D models. The difference among the three sensors is the geometry of the CSRRs: rectangular double-ring, circular double-ring and circular triple-ring. In the three cases, one of the resonators is loaded with the LUT placed in a capillary tube and serves as the sensing element, whereas the other one acts as the reference. The LUT container is placed through a hole etched in the center of the resonator. This region provides a strong electric field, which is necessary to achieve a high sensitivity, and a non-critical position for the tube in terms of manufacturing tolerances. The reference resonator is used to increase robustness against fluctuations in the environmental parameters, such as temperature and humidity, which might introduce errors. The effect of a change in the liquid composition is related to the difference of the two resonant frequencies observed in S_{11} and S_{22}.

The design of the sensors has been performed by EM simulations in CST Microwave Studio, by using the frequency domain solver. The substrate material is Rogers RO4003C, with a substrate thickness of 20 mil (0.508 m) and 35 μm-thick copper layers. Its permittivity and dielectric loss tangent are specified by the manufacturer as 3.38 ± 0.05 (process value)

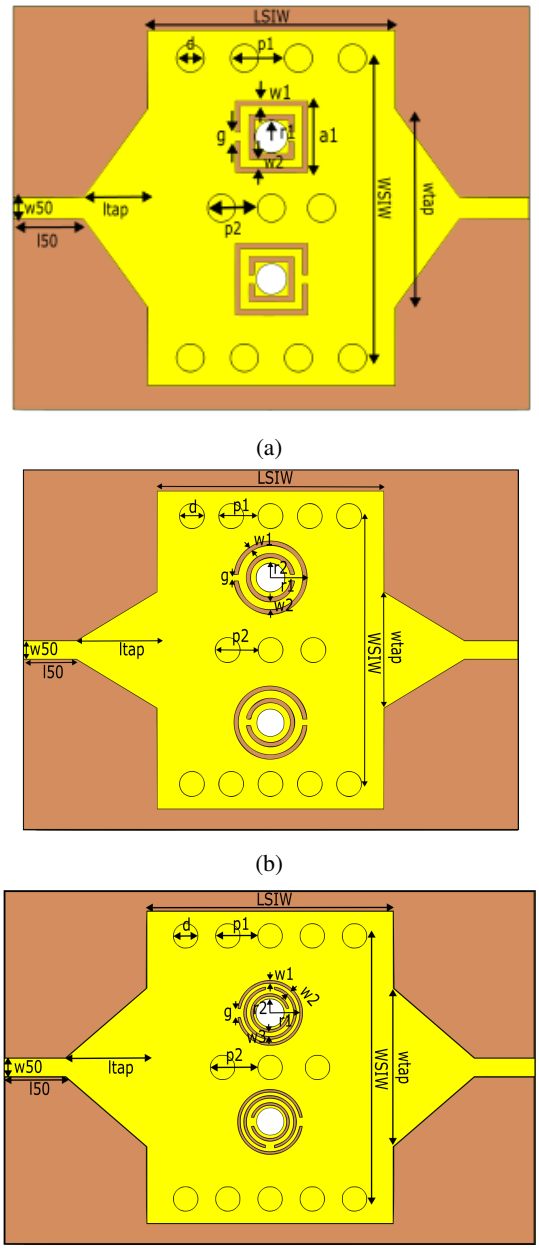

Fig. 1: Top views of the sensor models based on: double rectangular CSRRs (a), double circular CSRRs (b) and triple circular CSRRs (c).

and 0.0027, respectively, at 10 GHz. In CST, this dielectric substrate was simulated by using the available predefined material model. Using this model, CST calculates the dispersion characteristics of the substrate.

The feed structure consists of a microstrip taper and a 50 Ohm microstrip line section. The sensors are designed to operate in C-band, with resonance frequencies between 6 and 7 GHz for S_{11} without the liquid holder. The operation band has been selected to achieve a good compromise between compact size and manipulation ease in the lab, taking also layout restrictions into account. The specific geometrical parameter values are provided in Tables I to III. They were obtained by performing extensive parameter sweeps.

TABLE I: Geometrical dimensions of the sensor with double rectangular CSRR

Parameter	L_{SIW}	W_{SIW}	d	p_1	p_2	w_1	w_2
Value (mm)	12.40	13.57	1.40	2.70	2.50	0.25	0.44
Parameter	g	r_1	a_1	w_{50}	l_{50}	w_{tap}	l_{tap}
Value (mm)	0.45	0.805	3.60	1.05	3.50	9.90	3.20

TABLE II: Geometrical dimensions of the sensor with double circular CSRR

Parameter	L_{SIW}	W_{SIW}	d	p_1	p_2	w_1	w_2
Value (mm)	12.40	13.57	1.40	2.20	2.40	0.24	0.45
Parameter	g	r_1	r_2	w_{50}	l_{50}	w_{tap}	l_{tap}
Value (mm)	0.35	4.10	0.805	1.05	3.00	6.50	4.50

TABLE III: Geometrical dimensions of the sensor with triple circular CSRR

Parameter	L_{SIW}	W_{SIW}	d	p_1	p_2	w_1	w_2	w_3
Value (mm)	14.00	13.57	1.40	2.40	2.70	0.15	0.20	0.25
Parameter	g	r_1	r_2	w_{50}	l_{50}	w_{tap}	l_{tap}	
Value (mm)	0.50	3.70	0.805	1.05	3.50	9.00	4.60	

To investigate the sensitivity of the sensors, 3D models including the sensor structures together with capillary tubes containing samples, have been simulated in CST. The available capillaries were made of borosilicate glass, the interior diameter was specified between 1.1 and 1.2 mm, and the exterior diameter between 1.5 and 1.6 mm. For this material, a predefined model (named Schott Borofloat 33) available in CST was used. According to this model, between 6 and 7 GHz the real part of the permittivity is approximately 4.4 and the dielectric loss tangent ranges between 0.0066 and 0.0060.

Fig. 2 shows the results of the EM numerical simulations for different values of the LUT complex dielectric constant. In all the simulated cases, the reference tube is loaded with a liquid model, based on the water Debye model in CST. It can be seen that the real part of the LUT dielectric constant has a clear effect both on the resonant frequency and the notch depth. However, the dielectric loss mainly impacts the notch depth, having a negligible impact on S_{11} resonant frequency. It can also be observed that the LUT permittivity only has an impact on S_{11}, while S_{22} is not affected, because the reference liquid is the same and both CSRRs are uncoupled.

If environmental fluctuations were to produce a variation in the substrate relative permittivity, shifts of the resonant frequencies would be observed both in S_{11} and S_{22}, but the differential design would ensure robust operation. This is illustrated by an example in Fig. 3. In this case, the simulations have been performed using the water Debye model in the reference tube and a lossless LUT with a relative permittivity value of 30 in the other tube. It can be seen that the difference of S_{11} and S_{22} resonant frequencies remains constant.

Fig. 4 shows the top view of the sensor based on double circular CSRRs in CST, with the electric field distribution calculated at S_{11} and S_{22} resonant frequencies. It can be observed that the sensitivity of the circuit is based on the electric

This article has been accepted for publication in IEEE Sensors Journal. This is the author's version which has not been fully edited and
content may change prior to final publication. Citation information: DOI 10.1109/JSEN.2023.3332437

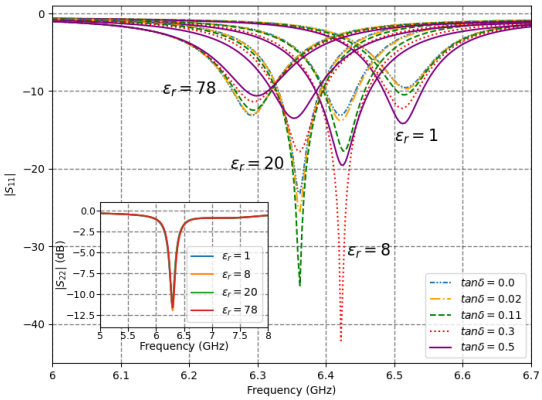

(a)

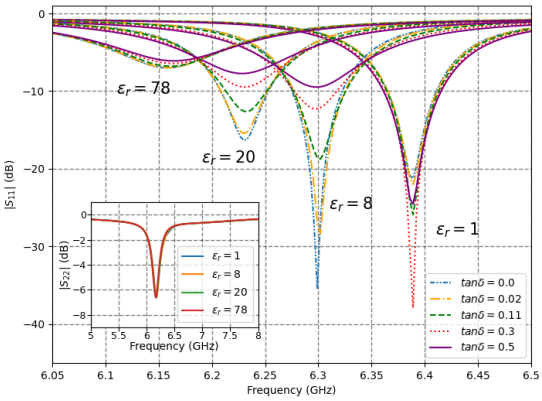

(b)

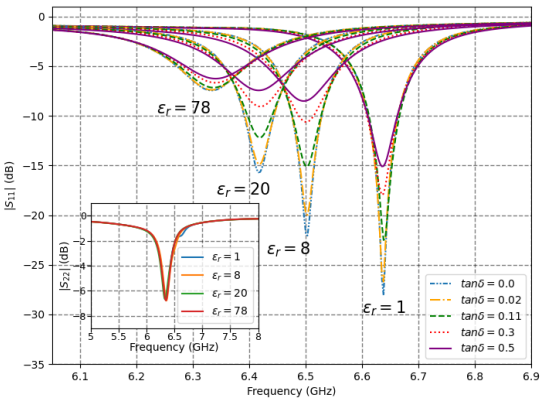

(c)

Fig. 2: Simulated S-parameters of the sensors for LUTs with different complex dielectric constants using the water Debye model in CST as the reference sample. The CSRR geometries are: double rectangular (a), double circular (b) and triple circular (c).

field concentration into a small area. The EM simulations also allowed to determine the minimum required volume of LUT. Taking into account the tube section and the height (protruding above and below the substrate) for which the electric field

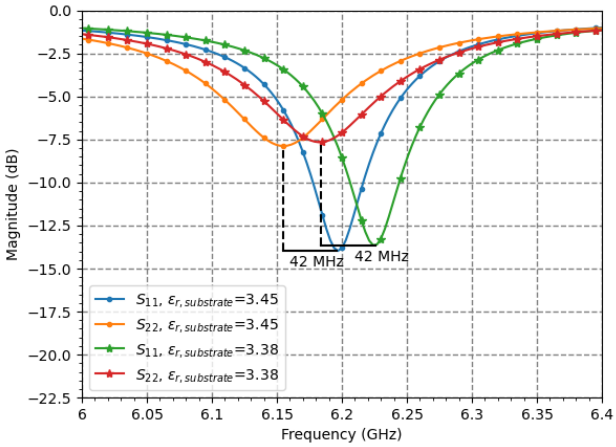

Fig. 3: Simulated S-parameters of the circular double-ring CSRR-based sensor for two different substrate permittivities. The simulated case corresponds to a lossless LUT, with $\epsilon_r = 30$, and the reference sample is the water Debye model in CST.

strength is reduced by 30 dB with respect to the maximum, it has been determined that the sensors are able to operate with a minimum liquid volume of about 1.5μL. The significant tube lengths are estimated by the EM simulations in 1.43, 1.37 and 1.28 mm for the sensors based on double rectangular CSRRs, double circular CSRRs and triple circular CSRRs, respectively. These values, used in the calculation of the minimum liquid volume, consider the field around the tube. Inside the tube, the lengths for an electric field strength reduction of 30 dB are lower in the three cases and have not been used in the calculation. The volume values obtained have been rounded up to the next integer multiple of 0.5μL resulting in 1.5μL.

III. Experimental Results

Three sensor prototypes have been manufactured and experimentally tested. First, the unloaded performance has been experimentally characterized to validate the numerical simulations, as explained in subsection III-A. After this validation, the sensors have been loaded with mixtures of DI-water and 96% medical ethanol to determine their average sensitivities. The results are described in subsection III-B.

A. Manufacturing and experimental validation of unloaded performances

The three sensors, including the via-holes, have been manufactured using an LPKF Protolaser S4 milling machine in standard PCB technology. Via-hole metalization was performed by inserting cylindrical copper rivets, that were crimped using a Bungard Favorit press tool. Fig. 5 shows the photograph of the three sensors, with the necessary connector footprints. The sensors were fed by solderless connectors (Rosenberg model 03K722-40MS3) and S-parameter measurements were obtained by using an N9918A Keysight Fieldfox Vector Network Analyzer (VNA).

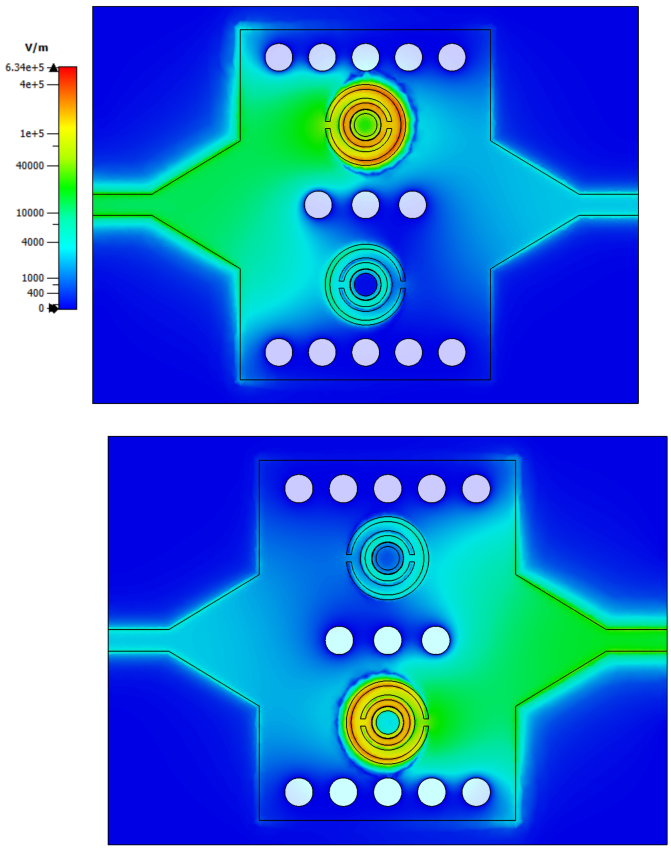

Fig. 4: Simulated electric field distribution of the circular CSRR-based SIW sensor at the resonance frequencies of S_{11} (upper plot) and S_{22} (lower plot).

First, the unloaded performance has been measured. Additional simulations were performed with CST after the prototypes had been realized to take the effect of the SMA connectors and the main tolerances into account. Some of the uncertainties come from the substrate tolerances. The considered substrate thickness was 0.508 ± 0.038 mm and the relative permittivity was 3.38 ± 0.05. Other factors that may lead to inaccuracies are related to the manufacturing process. In particular, the central holes in which the capillary tubes are inserted have been simulated using slightly tapered shapes instead of ideal cylinders to consider the laser defocusing effect across the substrate thickness. As for the plated via-holes, the impact of the tapered shape was proven to be negligible (0.045% change in S_{11} and S_{22} resonant frequencies), thus they were simulated as ideal cylinders. Finally, rounding effects have been considered in the worst-case analysis in the case of rectangular CSRRs taking the laser spot radius (10 μm) into account.

Fig. 6 shows the measured scattering parameters of the unloaded sensors with no liquid samples or containers in comparison to the simulated performances. The results of the worst-case analysis taking the parameter deviations into account are shown as grey areas in the three plots. As is clearly visible, the resonances in S_{11} and S_{22} parameters lie within the tolerance range. The slight asymmetries observed in the comparison of S_{11} and S_{22} parameters in this unloaded condition are attributed to manufacturing issues that may result in non-identical CSRRs.

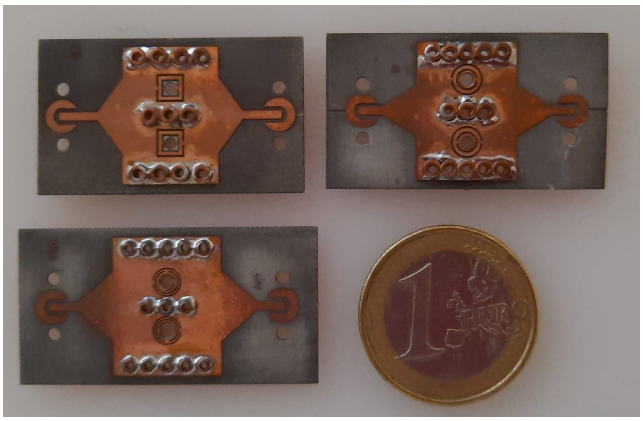

Fig. 5: Photograph of the three prototypes.

B. Experimental tests with binary liquid mixtures

In line with the scientific literature [34], mixtures of DI water and 96% ethanol have been used to test the sensitivity of the proposed sensors. The measurement set-up is shown in Fig. 7. The relative permittivity versus frequency of the liquid samples was previously measured using an open-ended coaxial probe from the N1501A Keysight Technologies kit and the VNA. The results are shown in Fig. 8, where $\epsilon_r^{'}$ and $\epsilon_r^{''}$ represent the real and imaginary parts of the complex dielectric constant, respectively. Fig. 9 shows the measurements of the sensors based on rectangular, double circular and triple circular CSRRs, respectively, when they were tested with DI water-ethanol mixtures with ethanol composition ranging from 0 to 100%. In the case of the triple-ring circular CSRR-based sensor, the prototype exhibited a reduced resonance depth and its performance, when loaded with the different mixtures, showed more fluctuations in the measurements and less stable resonance peaks than the other two sensors, based on double ring CSRRs. With a narrower distance between etched rings, and between the center hole and the first ring, we consider its manufacture more critical than the double circular geometry for this low-cost technology in this operation frequency band.

Different metrics have been used in the literature to characterize the sensitivity of liquid sensors. It is common that they are based on average values over the measured points, and usually they consider variations with respect to the unloaded case. Since the proposed design concept is differential, the frequency sensitivity is defined as the variation of the difference between the two notch frequencies (considering S_{11} and S_{22}) when the sensor is loaded with the LUT, with respect to the unloaded case (air), divided by the variation of the permittivity real part. Mathematically, this is expressed as:

$$f_d^{LUT} = f_{S_{22}}^{LUT} - f_{S_{11}}^{LUT} \tag{1}$$

$$f_d^{empty} = f_{S_{22}}^{empty} - f_{S_{11}}^{empty} \tag{2}$$

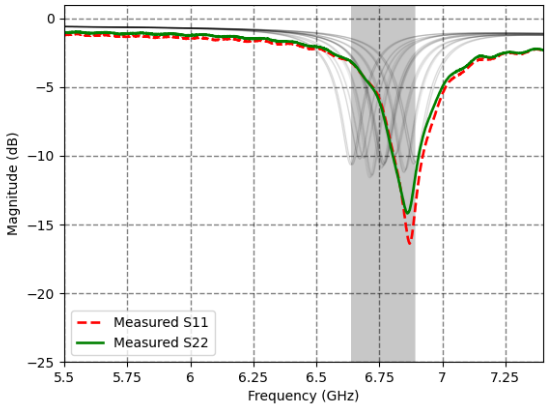

(a)

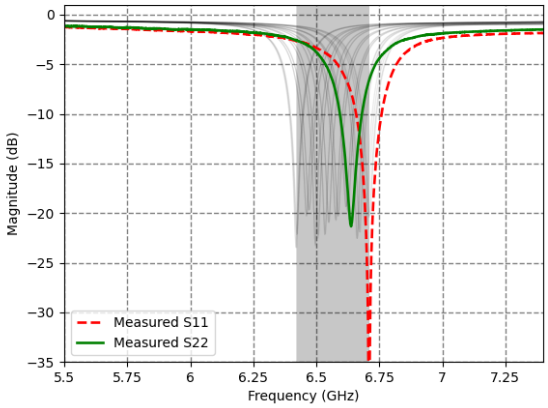

(b)

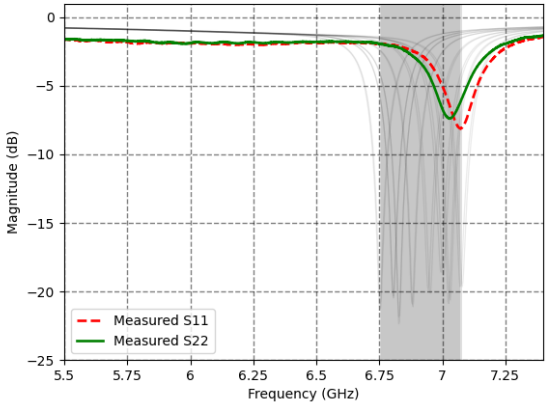

(c)

Fig. 6: Measured S-parameters of unloaded (no LUT/no tube) SIW sensors based on double rectangular CSRRs (a), double circular CSRRs (b) and triple circular CSRRs (c), versus simulated tolerance analysis (grey area).

$$S = \frac{\Delta f_d}{\Delta \epsilon_r^{'}} = \frac{f_d^{LUT} - f_d^{empty}}{\epsilon_r^{'LUT} - 1} \tag{3}$$

where $f_{S_{22}}^{LUT}$ and $f_{S_{11}}^{LUT}$ denote the resonance frequencies of S_{22} and S_{11}, respectively, when the sensor is loaded with

Fig. 7: Experimental setup consisting of a sensor with the sample holder connected to the VNA.

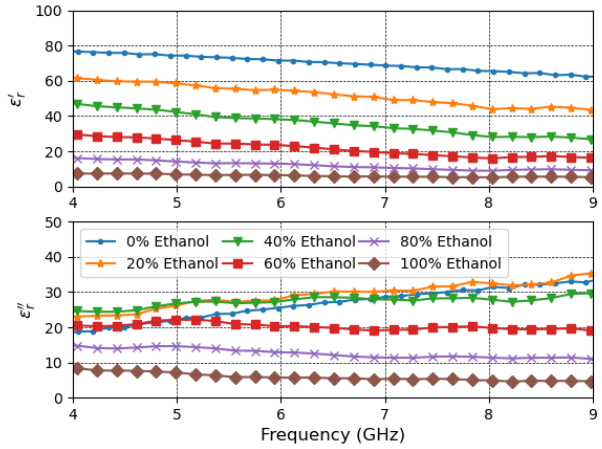

Fig. 8: Measured dielectric constant of ethanol-DI water mixtures performed with the open-ended coaxial probe.

the LUT in one tube and DI water in the second tube, and $f_{S_{22}}^{empty}$ and $f_{S_{11}}^{empty}$ denote the resonance frequencies when the tube dedicated to the LUT is empty whereas the reference tube contains DI water. Since it is a differential design, the reference tube contains DI water in both measurements. Therefore, $f_{S_{22}}^{LUT}$ and $f_{S_{22}}^{empty}$ are practically equal. $\epsilon_{LUT}^{'}$ is the real part of the relative permittivity of the LUT, determined by the open ended coaxial probe.

Dividing by $f_{S_{11}}^{empty}$, a relative sensitivity value is calculated, which can be expressed as a percentage as follows:

$$S_r = \frac{f_d^{LUT} - f_d^{empty}}{f_{S_{11}}^{empty}} \times \frac{1}{(\epsilon_{LUT}^{'} - 1)} \times 100\% \tag{4}$$

Table IV is a summary of the state-of-the-art regarding differential sensors based on frequency variation for liquid characterization. Let's denote by $S_{av}(MHz/\Delta\epsilon_r)$ the average frequency sensitivity and $S_{av,f}(\%)$ the average relative frequency sensitivity. The measured values of $S_{av,f}(\%)$ are 0.11, 0.18 and 0.09, for the sensors based on the double rectan-

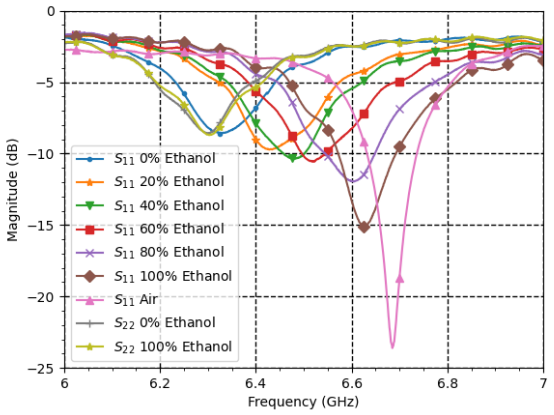

(a)

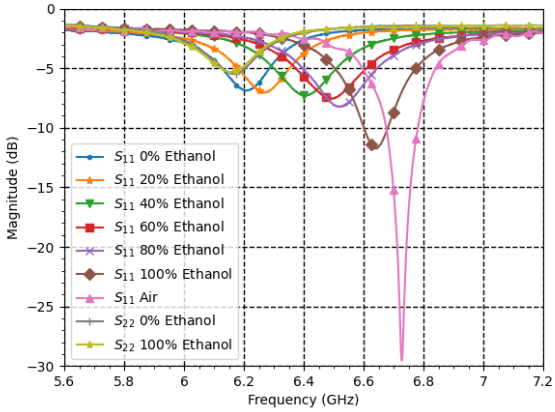

(b)

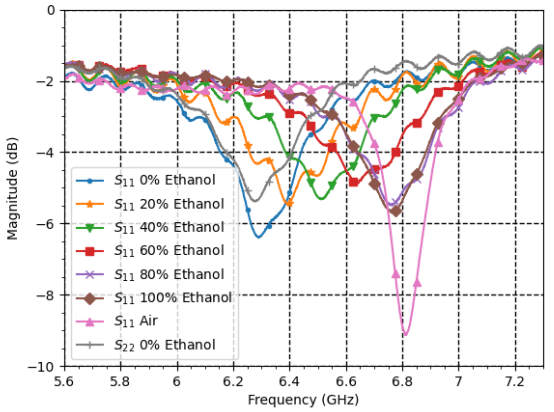

(c)

Fig. 9: Measured reflection coefficients of the rectangular (a), double circular (b), triple circular (c) CSRR-based sensor with ethanol-DI water mixtures. The sample in the reference tube is always DI water.

gular, double circular and triple circular CSRRs, respectively. Regarding $S_{av}(MHz/\Delta\epsilon_r)$, the measured values are 7.09, 12.24 and 6.10, respectively.

Comparison of the different sensors for liquid characterization presented in the scientific literature is not straightforward. The reason is that the experimental tests are not conducted under identical conditions. One of the factors is that the range of measured permittivity real part influences the calculation of the average sensitivity. For this reason, some authors [33] differentiate between permittivity regions with fast and slow sensitivities. The use of DI water-ethanol mixtures allows to cover a wide range of permittivity values and has become widespread. Another parameter that greatly affects the achieved sensitivity is the volume of liquid required. Both the range of measured permittivity real part and the minimum liquid volume required have been included in Table IV, in which f_0 denotes the resonance frequency of the sensor with air.

The best average sensitivity is obtained with the SIW sensor based on double circular CSRRs. The circular shape is considered more straighforward than the rectangular one because it matches the cross-section of the capillary tubes. Table IV shows that this sensor overcomes previous results obtained with differential designs in terms of $S_{av}(MHz/\Delta\epsilon_r)$. To demonstrate this sensitivity value, the sensor requires a very low sample volume. We have verified that the minimum sample volume (1.5µL) determined by EM simulations is experimentally valid by placing the capillary tube in positions for which only the significant heights, previously estimated with CST, protruded above or below the sensor. We checked that the measured performance was not modified with respect to a position of the tube more centered with respect to the substrate. Considering the sensitivity per unit volume of LUT as a figure-of-merit, the circuit demonstrates 8.2 MHz/$(\Delta\epsilon_r\mu L)$.

The measurements performed on DI water-ethanol mixtures allow to develop a mathematical sensing model to determine the percentage of ethanol in water from the sensor response. Using bivariate linear regression over the six measurement points, with Δf_d and the minimum S_{11} level (dBs) as the two variables, the coefficients of determination R^2 take values of 0.987, 0.974 and 0.960 for the sensors based on double rectangular, double circular and triple circular CSRRs, respectively, which represent a good linear fit.

IV. Conclusion

A novel design concept for planar microwave sensors implemented through three different layouts is proposed for liquid permittivity characterization. The circuits are based on SIW technology loaded with two CSRRs, with rectangular double ring, circular double ring and circular triple ring geometries. Under experimental tests based on DI water-ethanol mixtures, the best performance is achieved with the sensor based on circular double ring CSRRs. The main advantages are the high sensitivity per volume, robust operation based on a differential approach, and simple manufacturing and testing achieved through the use of two ports, PCB technology and no need of additional discrete surface-mounted componentes.

Future work can consider replacing the capillary tubes by microfluidic channels to obtain compact sensors with optimized performance based on the same design concept. The design of low-cost read-out circuits that avoid the need of the VNA is also an interesting task to address, which would open

TABLE IV: Comparison of differential sensors based on frequency variation for liquid characterization

Ref	Technology	f_0 (GHz)	$S_{av,f}$ (%)	$S_{av}(MHz/\Delta\epsilon_r^{'})$	Vol. (μL)	$\epsilon_r^{'}$ range	Size (mm^2)	No. ports	Discrete elements
[26]	OCSRR[1], microstrip	0.90	1.86	1.80	N.A.	25-80	26.0×70.0	4	No
[29]	CSRR, microstrip	1.62	0.63	10.14	N.A.	9-80	82.3×52.8	2	Yes
[35]	CSRR, microstrip	2.23	0.74	16.44	N.A.	1-80	90.0×60.0	2	Yes[2]
[28]	OCSRR, microstrip	2.35	0.88	20.73	0.91	10-80	20.0×52.0	2	Yes
[32]	CSRs, microstrip	1.02	0.28	2.86	1.56	15-80	30.0×30.0	2	No
[33]	Stepped-impedance, microstrip	2.45 5.80	0.05/0.02 0.04/0.02	1.11/0.51 2.35/1.18	4.0	1-30/30-80	40.0×30.0	2	No
This work	CSRR loaded SIW (double rectangular ring)	6.69	0.11	7.09	1.5	6-70	17.8×25.8	2	No
This work	CSRR loaded SIW (double circular ring)	6.73	0.18	12.24	1.5	6-70	17.8×27.7	2	No
This work	CSRR loaded SIW (triple circular ring)	6.81	0.09	6.10	1.5	6-70	17.8×30.2	2	No

[1] OCSRR stands for open CSRR.
[2] Discrete mounted elements for temperature compensation.

up the possibility of using this type of sensors autonomously in an internet-of-things context. Future research should also consider the realization of experiments focused on different specific applications.

REFERENCES

[1] M. R. Islam, M. T. Islam, A. Hoque, M. S. Soliman, B. Bais, N. M. Sahar, and S. H. Almalki, "Tri circle split ring resonator shaped metamaterial with mathematical modeling for oil concentration sensing," *IEEE Access*, vol. 9, pp. 161 087–161 102, 2021.

[2] R. K. Amineh, M. Ravan, and D. Tandel, "Detection of water pollutants with a nonuniform array of microwave sensors," *IEEE Transactions on Instrumentation and Measurement*, vol. 72, p. 6004011, 2023.

[3] P. Loutchanwoot and S. Harnsoongnoen, "Microwave microfluidic sensor for detection of high equol concentrations in aqueous solution," *IEEE Transactions on Biomedical Circuits and Systems*, vol. 16, no. 2, pp. 244–251, 2022.

[4] O. Peytral-Rieu, D. Dubuc, and K. Grenier, "Microwave-based sensor for the noninvasive and real-time analysis of 3-D biological microtissues: Microfluidic improvement and sensitivity study," *IEEE Transactions on Microwave Theory and Techniques*, 2023.

[5] J. Sorocki, K. Wincza, S. Gruszczynski, and I. Piekarz, "Direct broadband dielectric spectroscopy of liquid chemicals using microwave-fluidic two-wire transmission line sensor," *IEEE Transactions on Microwave Theory and Techniques*, vol. 69, no. 5, pp. 2569–2578, 2021.

[6] N. Hosseini and M. Baghelani, "Selective real-time non-contact multivariable water-alcohol-sugar concentration analysis during fermentation process using microwave split-ring resonator based sensor," *Sensors and Actuators A: Physical*, vol. 325, p. 112695, 2021.

[7] A. Ebrahimi, J. Scott, and K. Ghorbani, "Ultrahigh-sensitivity microwave sensor for microfluidic complex permittivity measurement," *IEEE Transactions on Microwave Theory and Techniques*, vol. 67, no. 10, pp. 4269–4277, 2019.

[8] L.-F. Chen, C. K. Ong, C. Neo, V. V. Varadan, and V. K. Varadan, *Microwave electronics: measurement and materials characterization*. John Wiley & Sons, 2004.

[9] F. Martín, P. Vélez, J. Muñoz-Enano, and L. Su, *Planar Microwave Sensors*. John Wiley & Sons, 2022.

[10] M. Abdolrazzaghi, N. Katchinskiy, A. Y. Elezzabi, P. E. Light, and M. Daneshmand, "Noninvasive glucose sensing in aqueous solutions using an active split-ring resonator," *IEEE Sensors Journal*, vol. 21, no. 17, pp. 18 742–18 755, 2021.

[11] O. Niksan, M. C. Jain, A. Shah, and M. H. Zarifi, "A nonintrusive flow rate sensor based on microwave split-ring resonators and thermal modulation," *IEEE Transactions on Microwave Theory and Techniques*, vol. 70, no. 3, pp. 1954–1963, 2022.

[12] M. S. Boybay and O. M. Ramahi, "Material characterization using complementary split-ring resonators," *IEEE Transactions on instrumentation and Measurement*, vol. 61, no. 11, pp. 3039–3046, 2012.

[13] E. L. Chuma, Y. Iano, G. Fontgalland, and L. L. B. Roger, "Microwave sensor for liquid dielectric characterization based on metamaterial complementary split ring resonator," *IEEE Sensors Journal*, vol. 18, no. 24, pp. 9978–9983, 2018.

[14] W.-J. Wu, W.-S. Zhao, D.-W. Wang, B. Yuan, and G. Wang, "Ultrahigh-sensitivity microwave microfluidic sensors based on modified complementary electric-LC and split-ring resonator structures," *IEEE Sensors Journal*, vol. 21, no. 17, pp. 18 756–18 763, 2021.

[15] D. Prakash and N. Gupta, "High-sensitivity grooved CSRR-based sensor for liquid chemical characterization," *IEEE Sensors Journal*, vol. 22, no. 19, pp. 18 463–18 470, 2022.

[16] A. Kandwal, Z. Nie, T. Igbe, J. Li, Y. Liu, L. W. Liu, and Y. Hao, "Surface plasmonic feature microwave sensor with highly confined fields for aqueous-glucose and blood-glucose measurements," *IEEE Transactions on Instrumentation and Measurement*, vol. 70, pp. 1–9, 2020.

[17] P. Velez, J. Munoz-Enano, A. Ebrahimi, C. Herrojo, F. Paredes, J. Scott, K. Ghorbani, and F. Martin, "Single-frequency amplitude-modulation sensor for dielectric characterization of solids and microfluidics," *IEEE Sensors Journal*, vol. 21, no. 10, pp. 12 189–12 201, 2021.

[18] L. Su, P. Vélez, P. Casacuberta, J. Muñoz-Enano, M. Gil-Barba, and F. Martín, "Reflective-mode phase-variation submersible sensor for liquid characterization," *IEEE Transactions on Instrumentation and Measurement*, vol. 72, 2023.

[19] A. H. Allah, G. A. Eyebe, and F. Domingue, "Fully 3D-printed microfluidic sensor using substrate integrated waveguide technology for liquid permittivity characterization," *IEEE Sensors Journal*, vol. 22, no. 11, pp. 10 541–10 550, 2022.

[20] N. Abd Rahman, Z. Zakaria, R. Abd Rahim, R. A. Alahnomi, A. J. A. Al-Gburi, A. Alhegazi, W. N. Abd Rashid, and A. A. M. Bahar, "Liquid permittivity sensing using teeth gear-circular substrate integrated waveguide," *IEEE Sensors Journal*, vol. 22, no. 12, pp. 11 690–11 697, 2022.

[21] G. M. Rocco, M. Bozzi, D. Schreurs, L. Perregrini, S. Marconi, G. Alaimo, and F. Auricchio, "3-D printed microfluidic sensor in SIW technology for liquids' characterization," *IEEE Transactions on Microwave Theory and Techniques*, vol. 68, no. 3, pp. 1175–1184, 2019.

[22] P. Mohammadi, H. Teimouri, A. Mohammadi, S. Demir, and A. Kara, "Dual band, miniaturized permittivity measurement sensor with negative-order SIW resonator," *IEEE Sensors Journal*, vol. 21, no. 20, pp. 22 695–22 702, 2021.

[23] J. Naqui, C. Damm, A. Wiens, R. Jakoby, L. Su, J. Mata-Contreras, and F. Martín, "Transmission lines loaded with pairs of stepped impedance resonators: Modeling and application to differential permittivity measurements," *IEEE Transactions on Microwave Theory and Techniques*, vol. 64, no. 11, pp. 3864–3877, 2016.

[24] P. Vélez, L. Su, K. Grenier, J. Mata-Contreras, D. Dubuc, and F. Martín, "Microwave microfluidic sensor based on a microstrip splitter/combiner configuration and split ring resonators (SRRs) for dielectric characterization of liquids," *IEEE Sensors Journal*, vol. 17, no. 20, pp. 6589–6598, 2017.

[25] A. Kumari, S. P. Singh, N. K. Tiwari, and M. J. Akhtar, "Design of a differential spoof surface plasmon sensor for dielectric sensing and defect detection," *IEEE Sensors Journal*, vol. 22, no. 4, pp. 3188–3195, 2022.

[26] P. Vélez, K. Grenier, J. Mata-Contreras, D. Dubuc, and F. Martín, "Highly-sensitive microwave sensors based on open complementary split ring resonators (OCSRRs) for dielectric characterization and solute concentration measurement in liquids," *IEEE Access*, vol. 6, pp. 48 324–48 338, 2018.

[27] A. Ebrahimi and K. Ghorbani, "High-sensitivity detection of solid and liquid dielectrics using a branch line coupler sensor," *IEEE Transactions on Microwave Theory and Techniques*, 2023.
[28] J. Yu, G. Liu, Z. Cheng, Y. Song, and M. You, "Design of OCSRR-based differential microwave sensor for microfluidic applications," *IEEE Sensors Journal*, vol. 22, no. 22, pp. 21 489–21 497, 2022.
[29] H.-Y. Gan, W.-S. Zhao, Q. Liu, D.-W. Wang, L. Dong, G. Wang, and W.-Y. Yin, "Differential microwave microfluidic sensor based on microstrip complementary split-ring resonator (MCSRR) structure," *IEEE Sensors Journal*, vol. 20, no. 11, pp. 5876–5884, 2020.
[30] A. Ebrahimi, F. J. Tovar-Lopez, J. Scott, and K. Ghorbani, "Differential microwave sensor for characterization of glycerol–water solutions," *Sensors and Actuators B: Chemical*, vol. 321, p. 128561, 2020.
[31] J. Naqui, C. Damm, A. Wiens, R. Jakoby, L. Su, and F. Martín, "Transmission lines loaded with pairs of magnetically coupled stepped impedance resonators (SIRs): Modeling and application to microwave sensors," in *2014 IEEE MTT-S International Microwave Symposium (IMS2014)*. IEEE, 2014, pp. 1–4.
[32] W.-J. Wu and W.-S. Zhao, "A differential THz/MW sensor for characterizing liquid samples based on CSRs," *IEEE Sensors Journal*, 2023.
[33] G. Acevedo-Osorio, E. Reyes-Vera, and H. Lobato-Morales, "Dual-band microstrip resonant sensor for dielectric measurement of liquid materials," *IEEE Sensors Journal*, vol. 20, no. 22, pp. 13 371–13 378, 2020.
[34] M. Chavoshi, M. Martinic, B. Nauwelaers, T. Markovic, and D. Schreurs, "Design of uncoupled and cascaded array of resonant microwave sensors for dielectric characterization of liquids," *IEEE Transactions on Microwave Theory and Techniques*, 2022.
[35] W.-J. Wu, W.-S. Zhao, D.-W. Wang, B. Yuan, and G. Wang, "A temperature-compensated differential microstrip sensor for microfluidic applications," *IEEE Sensors Journal*, vol. 21, no. 21, pp. 24 075–24 083, 2021.

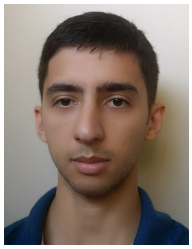

Víctor García received the Bachelor's Degree in Sound and Image Engineering in Telecommunication and the Master's Degree in Telecommunication Engineering from the Universidad de Extremadura (Spain) in 2019 and 2022, respectively. He is currently working as a predoctoral researcher at the Department of Computer and Communication Technologies, Universidad de Extremadura (Spain). His main research interest is the development of planar microwave sensors for dielectric characterization.

Yolanda Campos-Roca was born in Guitiriz (Lugo), Spain, in 1970. She received the M.S. and Ph.D. degrees in telecommunication engineering from the Universidade de Vigo, Vigo, Spain, in 1994 and 2000, respectively. Her Ph.D. dissertation concerned the design of millimeter-wave frequency multipliers. From 1996 to 2000, she performed research stays that accumulate almost three years at the Fraunhofer Institute for Applied Solid State Physics, Freiburg im Breisgau, Germany, either as a guest researcher affiliated to the University of Vigo or as a staff Member. In 2000, she joined the University of Extremadura, Cáceres, Spain, as an Assistant Professor, becoming an Associate Professor in 2002. Her current research interests include circuit design in the microwave, millimeter- and submillimeter-wave ranges and speech processing for biomedical applications.

Alfonso Gómez García was born in Córdoba, Andalusia, Spain in 1994. He received the M.S. and Ph.D. degrees with honors in telecommunication engineering from the University of Extremadura, Cáceres, in 2018 and 2023, respectively. For 5 years, he has collaborated as Professor Assistant with the Departamento de Tecnología de Computadores y Comunicaciones, University of Extremadura. Since 2023, he is employed as a Full-Time Researcher at the same institution. His research includes applications of a fast hybrid finite element/modal analysis method for microwave circuits and antennas, and the design and characterization of SIW based microwave antennas and circuits.